

EFFECT OF PRECURSOR CONCENTRATION AND pH ON THE SHAPE AND SIZE OF STARCH CAPPED SILVER SELENIDE (Ag_2Se) NANOPARTICLES

P. N. SIBIYA, M. J. MOLOTO*

Vaal University of Technology, Department of Chemistry, Private Bag X021,
Vanderbijlpark, 1900, South Africa

Water soluble starch capped silver selenide nanoparticles have been successfully synthesized at room temperature using sodium borohydride as a reducing agent. The effects of pH and precursor concentration were investigated for their influence on the size and shape of the synthesized nanoparticles. Starch is composed of acid and alcohol groups which can easily be influenced by change in pH. The chemistry of starch as polymeric has potential to stabilize nanoparticles. The nanoparticles have been characterized using UV-Vis spectroscopy, FT-IR spectroscopy, TGA, TEM, SEM and XRD techniques. The obtained nanoparticles gave particles size distribution ranging from 1 to 23 nm in diameter for all conditions used. The size of nanoparticles was found to decrease with an increase in pH 6 to 11, while the increase in precursor concentration (1:1, 1:2 and 2:1 of $\text{AgNO}_3:\text{Se}$) resulted in an increase in nanoparticle size.

(Received September 29, 2014; Accepted November 7, 2014)

Keywords: Silver selenide nanoparticles, Starch, Sodium borohydride, pH, Precursor concentration

1. Introduction

The use of nanoparticles, which are a group of atoms in the size range of 1–100 nm, is recently gaining momentum because they possess distinct chemical, optical and mechanical properties which cannot be shown by their bulk counterparts. These interesting properties of nanomaterials are strongly dependent on size, shape of nanoparticles and their interactions with stabilizers. For that reason it is a key challenge to control the synthesis of nanocrystals in order to achieve their useful characteristics [1]. The noble metals like silver and gold have drawn much attention due to their numerous applications in different branches including catalysis, photonics, photography and more significantly in the field of medicine as anti-microbial factors. Also, silver is of specific interest because of its unique properties, such as good conductivity, chemical stability, catalytic and antibacterial activity [2].

Among all semiconductor nanoparticles, metal selenides have been the subject of great focus due to their importance in various applications such as thermoelectric cooling materials, optical filters and sensors, optical recording materials, solar cells, superionic materials, laser materials and biological labels [3]. Silver selenide nanoparticles are known to possess good structural and electronic properties. As a semiconductor Ag_2Se has high electronic and ionic mobility [4]. Different methods have been used for the synthesis of high quality selenide nanoparticles. Low molecular weight molecules such as thiols, ethylhexanoate, polyphosphate and trioctylphosphine oxide have been used. However, the synthesis of selenide nanoparticles usually involves the use of high temperatures and reagents which are not environmentally friendly. These rigorous reaction conditions are toxic, volatile and explosive at elevated temperatures and thus are detrimental to the environment.

For these reasons there is an ongoing search for greener, sustainable and environmentally benign methods to synthesize these nanoparticles. In solution, bare nanoparticles are thermodynamically unstable, tend to aggregate and thus lose their peculiar properties. As a result

* Corresponding author: makwenam@vut.ac.za

of this, modification of the surface is essential for the prevention of uncontrolled growth and agglomeration of the nanoparticles. To prevent this agglomeration as well as the uncontrolled growth, capping agents are usually used. These capping agents are used as stabilisers to modify the surface of the nanoparticles and these include thiols, ethylhexanoate, polyphosphate, trioctylphosphine oxide (TOPO), polyesters and amino-derivatised polysaccharides. Among the materials used as stabilisers, polymers are mostly used because they provide an excellent steric hindrance effect with robust stability. Also, through hybridization with the polymers, nanoparticles are thought to inherit good compatibility, excellent capability as well as high engineering performance which are properties sought after in most technical applications of the nanoparticles [5].

In this study we report on the synthesis of starch capped Ag_2Se nanoparticles which have been synthesized using water to replace organic solvents at room temperature following Green chemistry principles. This has been undertaken because there has been a drive to refrain from the use of toxic chemical substances which are detrimental to the environment. The key issue in nanoscience research is to apply the principles of green chemistry principles to nanotechnology. It is essential not to use toxic chemicals in the synthesis process especially if the nanoparticles have the potential to be used in medical applications in order to avoid any adverse effects to people and the environment [6]. Starch has been used as a capping agent because it environmentally friendly, biocompatible and can be easily modified for a wide range of potential applications.

The work is focused on investigating the effect of pH and precursor concentration on the size, optical and morphological properties. It is envisaged that the insight gained from this green synthetic approach will enable an economically feasible and environmentally friendly method for the synthesis of modified water soluble nanoparticles.

2. Methodology

2.1 Chemicals

Silver nitrate (AgNO_3) (99%), ammonium hydroxide (NH_4OH) (99.9%), selenium powder (99.5%, 100 mesh) sodium borohydride (NaBH_4) (98.5%), soluble starch (99.9%) were purchased from Merk (Germany). All chemicals were used as purchased.

2.2 Synthesis of starch capped Ag_2Se nanoparticles

The methodology used for the synthesis of Ag_2Se nanoparticles in aqueous phase was adopted from Oluwafemi et al. [7], with slight modifications. Selenium precursor solution was prepared by adding (0.32–0.64 mmol) selenium powder to (20 mL) deionised water in a three-necked flask at room temperature. To this reaction mixture sodium borohydride (0.81 mmol) was then added and the flask was immediately purged with nitrogen gas to create an inert atmosphere. The reaction mixture was further stirred for 2 h at room temperature. The starch capped silver selenide nanoparticles were prepared by adding 1.0 mL solution of silver nitrate (0.32–0.64 mmol) to 20 mL soluble starch solution (0.05%) in a one-necked round-bottom flask. The mixture was constantly stirred at room temperature. The pH of the solution was adjusted from 6–11 using (0.1M) ammonium hydroxide. A colourless selenide ion solution (1.0 mL) was then added and the reaction mixture was further stirred for 20 hours at room temperature. At the end of the reaction solution was centrifuged and extracted with acetone to obtain a grey-black precipitate of Ag_2Se nanoparticles. The precipitate was washed and then dried at room temperature.

2.2.1. Effect of pH

The pH has a significant influence on both the size and the crystallinity of the nanoparticles. In order to investigate the effect of pH on the size of the synthesized nanoparticles, experiments were prepared at acidic (without ammonium hydroxide), neutral and basic medium adjusted with ammonium hydroxide. Conditions of the study are presented in Table 1. The samples were analysed using UV-Vis spectroscopy, FT-IR spectroscopy and TEM.

2.2.2. Effect of precursor concentration

The concentration of the precursor is responsible for the morphology and size of nanoparticles. To investigate the effect of the precursor concentration on the size and morphology of the synthesized nanoparticles, different concentration ratios of silver nitrate salt and selenide powder (1:1, 1:2 and 2:1) were utilized. The resultant nanoparticles were analysed with UV-Vis spectroscopy, FT-IR spectroscopy, TEM, XRD, TGA and SEM instruments. The conditions (pH and precursor concentrations) investigated are shown in **Table 1**.

Table 1: Variation of reaction parameters

Sample	pH	Precursor conc. (ratio)
A	6	1:1
B	7	1:1
C	11	1:1
D	11	1:2
E	11	2:1

2.3 Characterisation

A Perkin Elmer Lamda 25 UV-Vis Spectrophotometer was used to carry out all optical studies. The measurements were performed in the 200-1100 nm wavelength range and at room temperature. To perform the analyses, the samples were placed in quartz cuvettes cell of 1 cm path length. Fourier transform infrared (FT-IR) analyses were carried out using a Perkin Elmer spectrum 400 FT-IR-NIR Spectrometer equipped with a universal ATR sampling accessory. To study the microstructure of the nanoparticles, a JEOL JEM-2100 transmission electron microscope operating at 200 kV was used. The TEM was coupled with an energy dispersive X-ray (EDX) detector and was also used to determine the elemental composition of the synthesized nanoparticles. For analysis, the samples were prepared by putting an aliquot solution of the water soluble nanocrystalline material onto an amorphous carbon substrate supported on a copper grid and then the solvent was allowed to evaporate at room temperature.

To analyze and visualize the surface morphology of the nanoparticles, a quanta VEGA 3 TESCAN scanning electron microscope (SEM) was used. For SEM analysis, the samples were placed on a carbon tape and analyzed without gold coating. The X-ray diffraction patterns were recorded by a Bruker D2 diffractometer at 40 kV and 50 mA. A secondary graphite monochromated Co K alpha radiation ($\lambda = 1.7902 \text{ \AA}$) was used and the measurements were taken at high angle 2θ in a range of 5° - 90° with a scan speed of $0.01^\circ 2\theta \text{ s}^{-1}$. For thermal analysis a Perkin Elmer Thermogravimetric Analyzer (TGA 4000) was used. The samples were heated under nitrogen and the heating range was between 25 and 900 °C at a heating rate of 5°/min.

3. Results and Discussion

3.1 Reaction mechanisms

The overall chemical reaction involved in the synthesis of starch-capped nanoparticles can be represented by the following equations:



The whole process is a redox reaction where selenium acts as the oxidant and Ag_2Se as the reduction product. NaBH_4 acts as the reducing agent and $\text{Na}_2\text{B}_4\text{O}_7$ should be the oxidation product. In the experiments, Se is reduced to NaHSe as NaBH_4 is oxidised to $\text{Na}_2\text{B}_4\text{O}_7$. AgNO_3 reacts with starch to form starch-silver complex, which then reacts with Se^{2-} to form starch-capped Ag_2Se nanoparticles. The OH groups of starch thus act as coordination sites for the release of the metal ions and thus control the chemical reaction rate of the combination of Ag^+ and Se^{2-} to produce MSe nanoparticles [7], [8].

3.1.1 Optical analysis of starch-capped Ag_2Se nanoparticles

(a) Effect of pH

Fig. 1 shows the absorption spectra of starch capped silver selenide nanoparticles synthesized at pH 6, 7 and 11 with starch (0.05 wt%) and 0.32 mmol monomer (Ag and Se) concentrations were used for the synthesis of the Ag_2Se nanoparticles. The pH was observed to play a significant role in influencing the size of the nanoparticles. This is because pH affects the distribution of starch hydroxyl groups which in turn affects the size of the nanoparticles. Lower pH causes change in the chemical structure and activity of starch due to formation of alkoxide and carboxylate ions. It is noteworthy that increasing the pH value enhances the percentage of starch hydroxyl group species thus resulting in smaller sized nanoparticles [9]. From **Figure 1** it can be seen that the spectra obtained at pH 6 and 7 gave no excitonic shoulders, while a distinct excitonic shoulder appeared at a wavelength of 470 nm for pH 11 which is an indication of the monodispersity of the particles. The absorption peak is blue-shifted from the bulk band gap of silver selenide which is 1033 nm, indicating the formation of nanoparticles. There is however no distinct difference between the graphs at pH 6 and pH 7. The reason could be that the addition of ammonium hydroxide at pH 7 was minimal hence the effect of the ammonium hydroxide might be negligible. From the results obtained in this work, it was found that alkaline pH is more suitable for synthesis of silver selenide nanoparticles, which is in agreement with other research findings [10]. The higher peak absorbance at pH 11 also indicate higher amount of nanoparticles produced, which was confirmed by TEM results [2]. It was then chosen as the best pH for the synthesis of starch capped silver selenide nanoparticles.

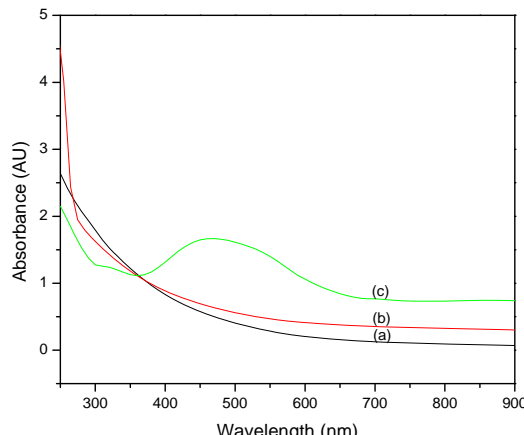


*Fig. 1: UV-Vis absorption spectra of starch capped Ag_2Se prepared using AgNO_3 and selenium (1:1) at (a) pH 6, (b) pH 7 and (c) pH 11 with 0.05 w% starch.
(b) Effect of precursor concentration*

Figure 2 shows the absorption spectra of starch capped silver selenide nanoparticles prepared using different concentrations at pH 11. The capping agent (starch) was kept at 0.05 wt%. The absorption spectra at 1:1, 1:2 and 2:1 molar ratios showed an absorption shoulder at 470 nm (1.05 eV), 480 nm (eV) and 470 nm (1.13 eV), respectively which were all shifted from the bulk band gap of silver selenide (0.07-0.15 eV) as a result of quantum confinement. The broadness of the absorption shoulder for (1:2 and 2:1) ratios could be attributed to the self-assembly of the nanoparticles or the formation of bigger particle size [7], [10].

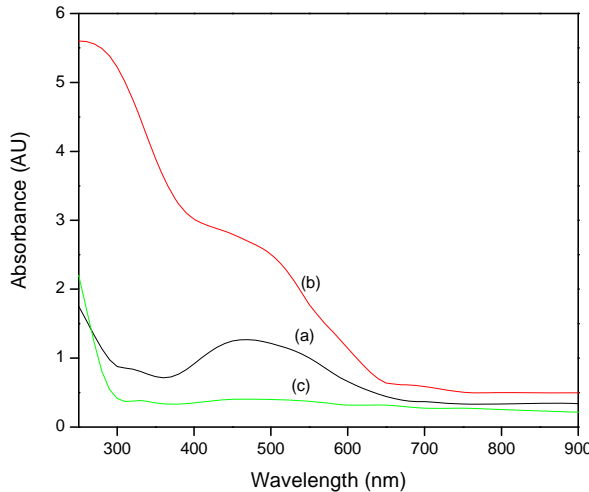


Fig. 2. UV-Vis graph for starch capped Ag_2Se nanoparticles: (a) 1:1, (b) 1:2 and (c) 2:1 $\text{AgNO}_3:\text{Se}$, at pH11 with 0.05 w% starch.

3.1.2 FT-IR spectral analysis

The surface chemistry of the synthesized materials was investigated using FT-IR spectroscopy. Figure 3 shows the IR spectra of starch capped silver selenide nanoparticles at different precursor concentrations, synthesized with starch 0.05 wt% of starch at pH11. Figure 4 shows FT-IR spectra of starch capped silver selenide nanoparticles at different pH. The spectra showed an intense broad band at 3295 cm^{-1} which is attributed to the O-H stretching of starch and its width was attributed to the formation of inter and intramolecular hydrogen bond. The asymmetric stretching of C-H band was observed at 2930 cm^{-1} while the band at 1643 cm^{-1} was attributed to water adsorbed in the amorphous region of starch. The band at 1415 cm^{-1} was due to both the CH_2 bending and the C-O-O stretch. The band at 1337 cm^{-1} was assigned to the angular deformation of C-H, while at 1244 cm^{-1} is a CH_2OH (side chain) related mode. The two characteristic bands at the fingerprint region of spectra at 1149 cm^{-1} and 1076 cm^{-1} were attributed to the C-O, C-C stretching and C-O-H bending of starch, respectively. The prominent band at 996 cm^{-1} was attributed to the skeletal mode vibration of α 1,4-glycosidic linkage (C-O-C) while the band at 762 cm^{-1} was attributed to C-C stretching [7], [11-13].

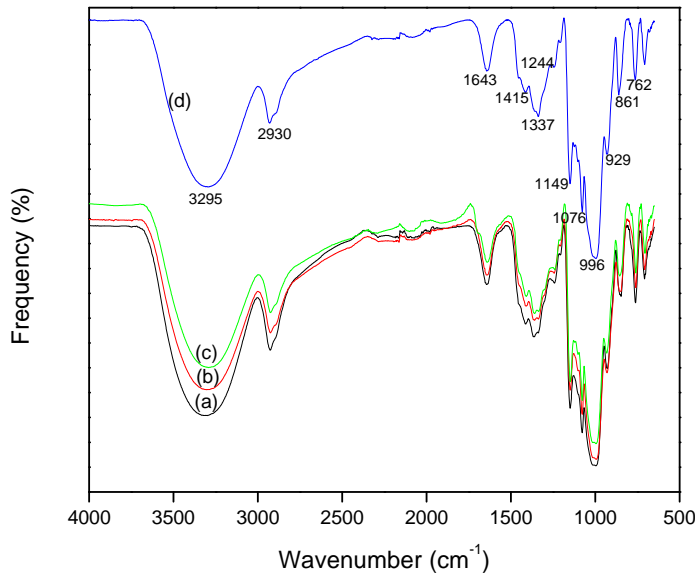


Fig. 3. FTIR spectra of starch capped Ag_2Se nanoparticles prepared at pH 11 with 0.05 w% starch: (a) 1:1, (b) 1:2, (c) 2:1 $\text{AgNO}_3:\text{Se}$ and (d) pure starch

On the investigation of the effect of pH, the spectra showed that the band which is due to OH stretching is less intense under acidic conditions (Fig. 4a). The reason for this could be that in acidic pH, the association between the functional groups of starch through H-bonding is likely to be more prominent, this then stabilizes the structures resulting in starch not being effectively utilized in the reduction process [14]. This phenomenon is reversed by increasing the basicity of the condition, which is the reason why basic pH 11 (Fig. 4b) gave enhancement in the plasmon intensity of the UV-Vis (Figure 1) indicating the production of large amounts of silver ions that are reduced in size which is further confirmed by TEM results (Figure 6). At neutral pH (Figure 4c), the intensity of the OH band is more intense. The reason for this could be that the secondary alcoholic groups of starch was oxidized to keto group which could be verified by an intense band at 1644 cm^{-1} due to the bending vibration of OH group of starch [15]. By analyzing the FTIR results one can come to a conclusion that during alkaline treatment there will be conversion of secondary alcoholic group into a keto group at neutral pH. The starch characteristic bands were present in all the synthesized nanoparticles which confirmed the capping of the nanoparticles with starch. The shift in the wavenumber of the OH group and CH_2OH side chain on the starch capped nanoparticles was due to the binding of starch with the metal.

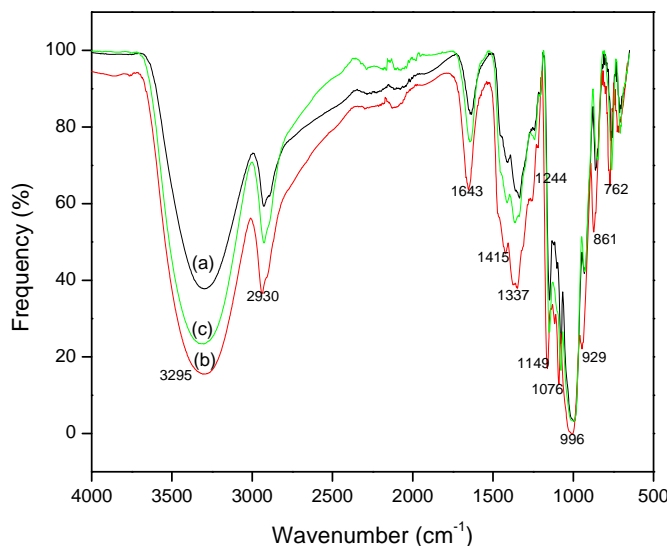


Fig. 4 FTIR spectra of starch capped Ag_2Se nanoparticles prepared with $\text{AgNO}_3:\text{Se}$ (1:1) and 0.05 w% starch at (a) pH 6, (b) pH 7 and (c) pH 11

3.1.3 TGA Analysis

The TGA plot of starch capped silver selenide nanoparticles is shown in Fig. 5. The first degradation step observed below 100 °C was due to desorption of water from the nanoparticles. The second degradation step was due to the decomposition of starch leaving behind Ag₂Se nanoparticles. This was observed at 310 °C for 1:1 ratio, 296 °C for 1:2 ratio and 319 °C for 2:1. However, it is important to note that there is no endothermic peak observed in the derivative curve which is an indication that there is no further chemical or physical change occurring to the nanoparticles. The TGA graphs show no further weight loss above 319 °C which can be attributed to the high thermal stability of these nanoparticles. The TGA results thus revealed that the stability of the nanoparticles is dependent on the ratio of silver to selenide. It can be concluded that as the amount of silver increases the stability of the nanoparticles also increases (1:2 or 0.5:1 < 1:1 < 2:1).

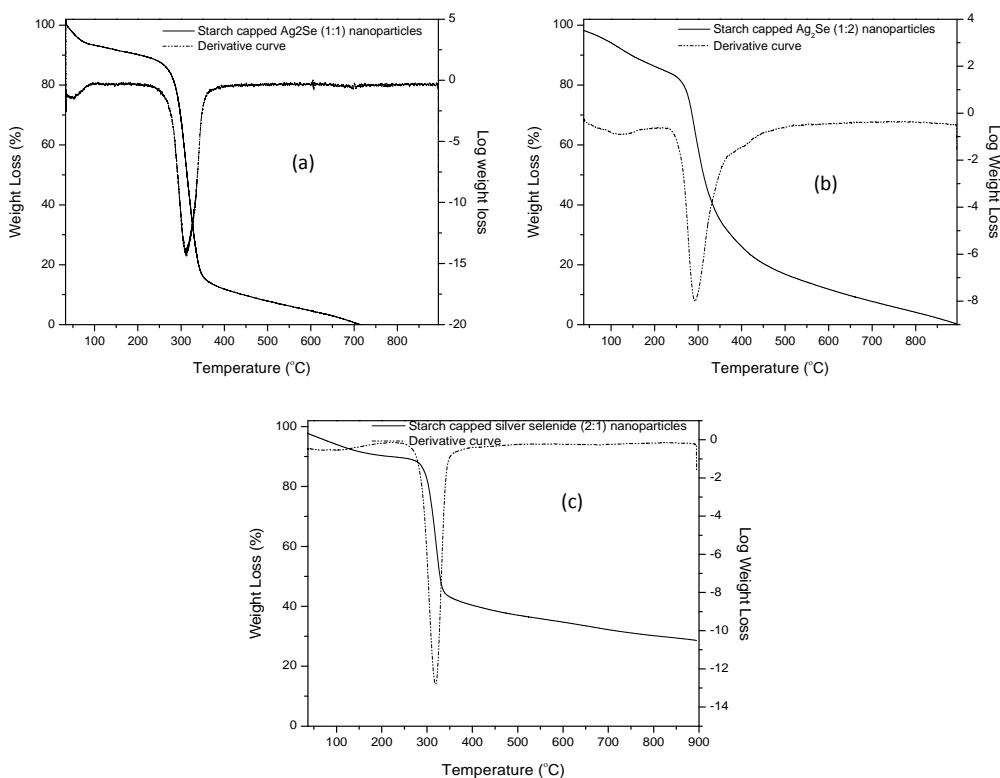


Fig. 5. TGA thermograms of starch capped Ag₂Se nanoparticles at pH 11 with 0.05 w% starch, a) 1:1, b) 1:2, c) 2:1 AgNO₃:Se.

3.1.4 TEM analysis

(a) Effect of pH

The TEM micrographs of the nanoparticles formed using the three different pH values are shown in Fig. 6. From the TEM images it can be observed that nanoparticles obtained at pH 6 and pH 7 showed fewer nanoparticles with bigger particle sizes. Increasing the pH resulted in reduced nanoparticle sizes. A similar pattern has been reported by [9] where they investigated the effect of pH on silver nanoparticles. The mean particle sizes estimated from the TEM images were found to be 5.76 nm (pH 6), 7.90 nm (pH 7) and 1.92 nm (pH 11).

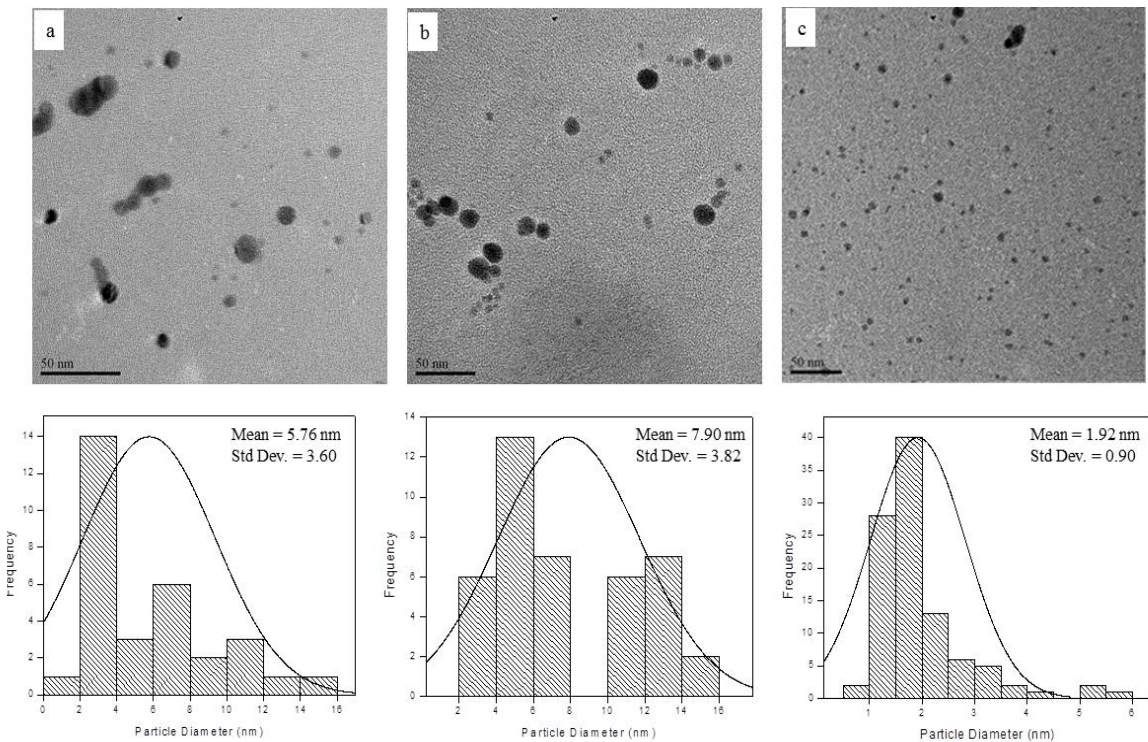


Fig. 6. TEM micrographs of starch capped Ag_2Se (1:1), at pH 6, 7 and 11 with 0.05 w% starch.

(b) Effect of precursor concentration

Fig. 7 shows the nanoparticles produced as a function of varying the precursor concentration. The nanoparticles obtained showed an increase in particle size with increase in precursor concentration. The average nanoparticle sizes estimated from the TEM images were found to be 1.92 nm (1:1), 4.44 nm (1:2), 5.30 nm (2:1) and 23.58 nm (1:10). The reason for this could be that the presence of large amount of precursor created high attraction between silver and selenide atoms. This resulted in the agglomeration of nanoparticles and thus the formation of particles with large size. A similar trend has also been observed and reported by Sofekordi et al., (2011). The reason for the increase in nanoparticle size might have arisen from the same wt % of starch (0.05) used for the different concentration ratios which may not have been sufficient for effective passivation at higher concentration.

The 1:1 ratio showed spherical, numerous well dispersed nanoparticles and the 1:2 ratio showed spherical, fewer well dispersed nanoparticles which indicate that the lower the concentration of silver the lower the production of nanoparticles. The 2:1 ratio showed spherical, numerous closely packed nanoparticles. To further understand the effect of concentration a higher concentration (1:10) ratio was used. The spherical particles and larger rod shape particles were observed, which indicated that the precursor concentration has an effect on the size of nanoparticles. This could also mean that the wt% of the starch used greatly influenced the transformation of the nanoparticle shape from spherical to rod. The large size and aggregation of nanoparticles was observed with increase in precursor concentration and this could be due to the increase in silver ions that compete with functional groups of the capping agent [10]. Different patterns were also observed from TEM images as the spherical particles arranged themselves into elongated ones. The patterns observed included tripods, sinusoidal and S-shaped nanoparticles, which indicated that the self-reorganisation occurred via the bonding between the spherical nanoparticles due to dipole-dipole interactions between the highly charged surfaces of II-VI semiconductor nanocrystals [7].

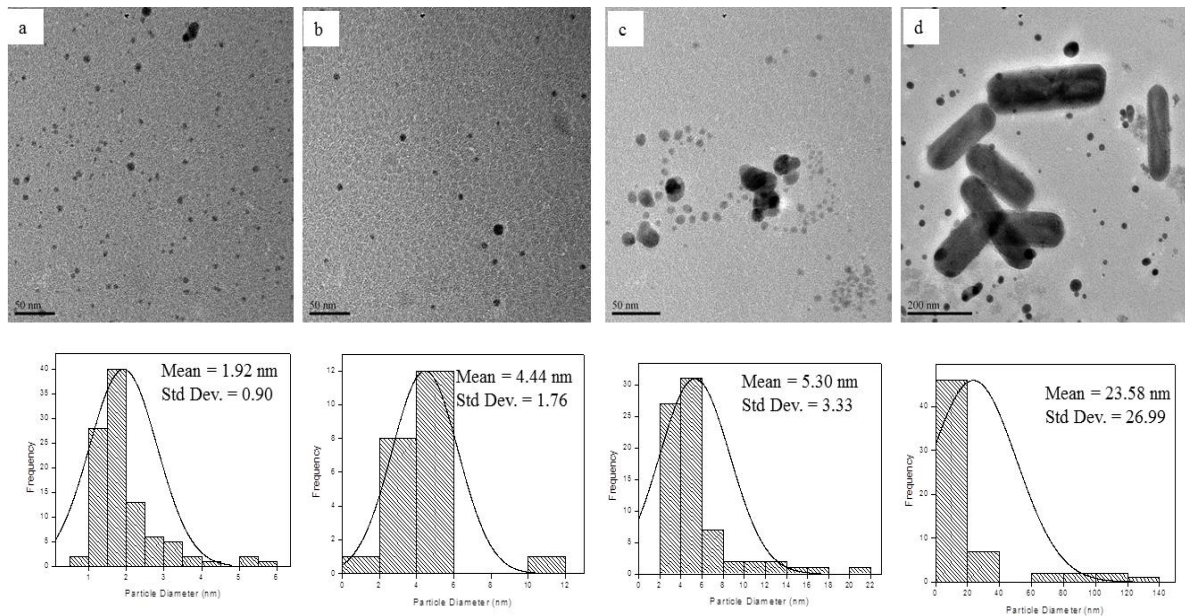


Fig. 7. TEM images for starch capped Ag₂Se nanoparticles with 0.05 w%/starch at pH 11: a) 1:1, b) 1:2, c) 2:1 and d) 1:10

3.1.5 EDX Analysis

The elemental composition of the prepared nanoparticles was studied using energy dispersive X-ray (EDX) spectroscopy. The EDX spectrum of silver selenide nanoparticles is shown in Fig. 8. The EDX profile showed the presence of both elemental silver and selenide peaks. The presence of the carbon and the copper peaks was due to the adhesion of carbon tape and copper grid, respectively. The observed chromium and iron peaks were from the sample holder. Identification lines for the major emission energies for silver was observed in the range 2.5 - 4 keV, selenium was observed in the range of 1.2 - 1.6 keV and 10.6 - 13 keV. These observed peaks observed in the spectrum conform to those previously identified [16](Ajitha et al., 2013). Thus reduction of silver into elemental silver and selenium has been confirmed by the EDX studies. Ag and Se in the proportion 2:1, thus suggesting the formula Ag₂Se.

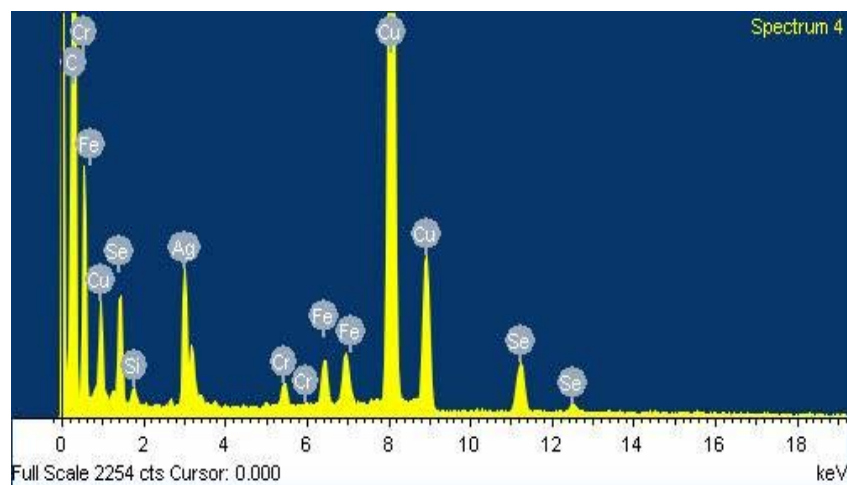


Fig. 8. A typical EDX spectrum of starch capped silver selenide (1:1) nanoparticles with 0.05 w% starch at pH 11.

3.1.6 SEM Analysis

The surface morphology of the nanoparticles were studied. Fig. 9 illustrates the SEM micrographs of starch capped Ag₂Se nanoparticles. The SEM analyses revealed that nanoparticles made were spherical in shape. SEM images micrographs also showed that the nanoparticles were homogeneous and without any substantial agglomeration. The results obtained from these SEM studies was found to be in agreement with the results obtained with the TEM studies.

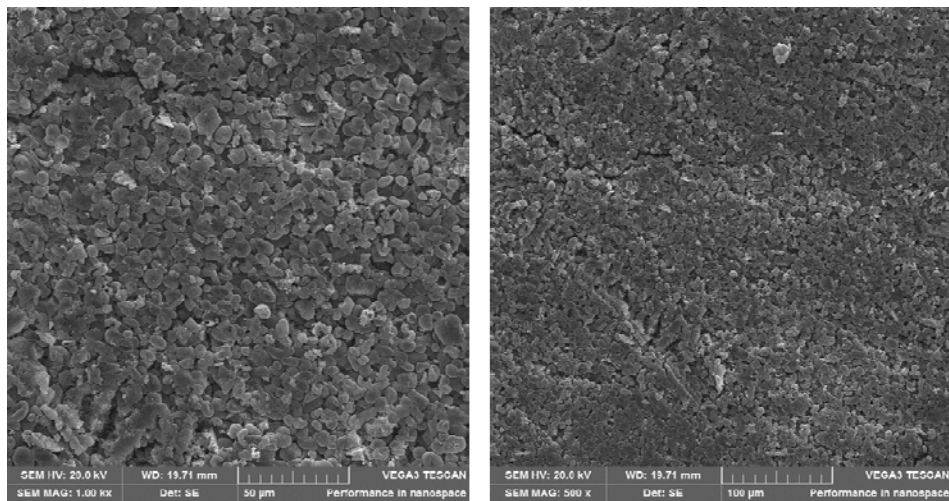


Fig. 9. SEM micrographs of starch capped Ag₂Se (1:1) nanoparticles at pH 11

3.1.7 XRD Analysis

Ag₂Se exist in two polymorphs at atmospheric pressure: there is a low-temperature orthorhombic phase (β -Ag₂Se) below 133 °C and a high temperature cubic phase (α -Ag₂Se) above 133 °C [17]. The diffraction peaks of the products in Fig. 10 can be indexed to orthorhombic phase Ag₂Se (JCPDS card 03-065-2625).

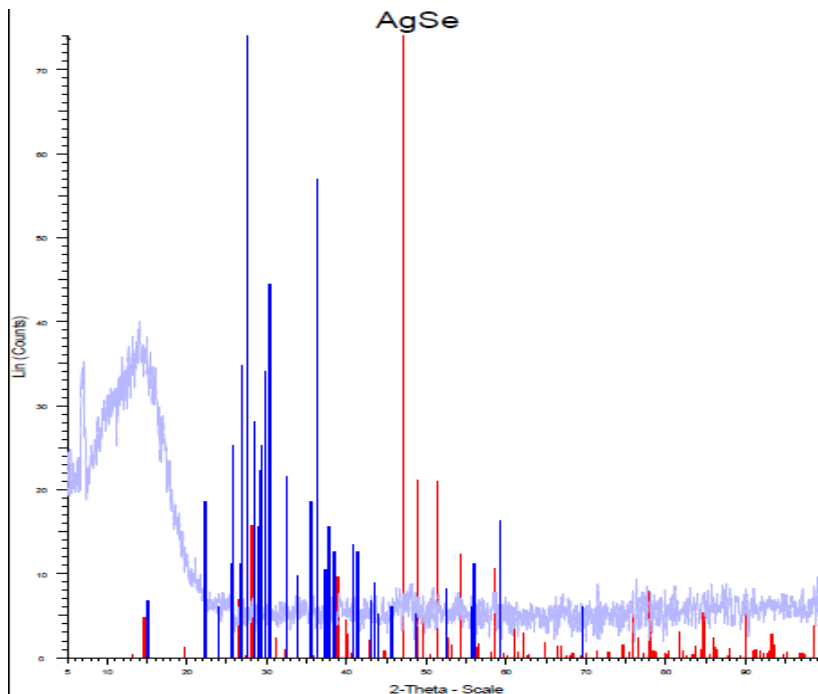


Fig. 10. XRD micrographs of starch capped Ag₂Se (1:1) nanoparticles at pH 11

Precursor concentration is a critical parameter that impacts the size and the morphology of the nanoparticles. It has also been reported that using high concentrations of precursor extends the time taken for the growth of the particles thus resulting in varying morphologies. The pH plays a significant role in influencing the size of the nanoparticles. This is because pH affects the distribution of starch hydroxyl groups which in turn affects the size of the nanoparticles. Increasing the pH value enhances the percentage of starch hydroxyl group species thus resulting in smaller sized nanoparticles [9], [18]. Due to the above mentioned reasons, the effect of precursor concentration and pH were investigated in this work.

4. Conclusion

In this research work, the production of starch capped silver selenide nanoparticles in different conditions was studied. The effect of pH and precursor concentration on the production of silver selenide nanoparticles was studied. The reason for studying these quantities was to achieve optimal and suitable conditions for the production of silver selenide nanoparticles. The present investigation indicated that alkaline pH is more suitable for synthesis of silver selenide nanoparticles. The increase in precursor concentration showed an increase in nanoparticle size and further increase results in change in particle shape. TGA results showed that 2:1 precursor ratio is the most stable. SEM and TEM results showed that the nanoparticles obtained are spherical in shape without major agglomeration and they formed rod shape at higher precursor concentration. XRD and EDX results indicated that Ag₂Se nanoparticles have been successfully obtained in this work.

Acknowledgements

The authors are greatful to Vaal University of Technology (VUT) research directorate and the department of chemistry for funding, laboratory support and research infrastruture used for carrying out the research work.

References

- [1] A.A.El-Kheshen, S.F.D. El-Rabi, Der Pharma Chemica. **4**(1), 53 (2012).
- [2] A.A.Safekordi, H. Attar, H.R.Ghorbani International Conference on Chemical, Ecology and Environmental Sciences. 346-350. 2011.
- [3] S.R Devi, R.K.L Singh, S.S. Nath Chalcogenide Letters. **10**(4), 151 (2013).
- [4] M. Jafari, M. Salavati-Niasari, Nanomaterials: Applications and Properties **2**(2), 02PCN49 1-3. (2013).
- [5] A.F. Abouraddy, M. Bayindir, G.T. Benoit Nat. Mater. **6**, 336 (2007).
- [6] P. Raveendran, J. Fu, S.L. Wallen J. Am. Chem. Soc. **125**, 13940 (2003).
- [7] O. S. Oluwafemi, N. Revaprasadu Mater. Res. Soc. Symp. Proc. **1138**, 12 (2009).
- [8] P. Mishra, R.S. Yadav, A.C. Pandey Digest. J. Nano. Bios. **4**, 193 (2009).
- [9] K. Mahdi, G.Sayed Ali Akbar, A.Mohammad Ali, Iran. J. Chem. Chem. Eng. **31**(4), 21 (2012).
- [10] M. Vanaja, S. Rajeshkumar, K. Paulkumar, G. Gnanajobitha, C. Malarkodi, G. Annadurai Advances in Applied Science Research. **4**(3), 50 (2013).
- [11] N. Santha, K. G. Sudha, K. P. Vijaykumari, V.U. Nayar, S. N. Moorthy Proc. Indian Acad. Sci. (Chem. Sci.). **102**, 705 (1990).
- [12] R. H. Wilson, B. J. Goodfellow, P. S. Belton, B. G. Osborne, G. Oliver, P. L. Russell, J. Sci. Food Agric. **54**, 471 (1991).
- [13] J. J. Cael, J. L. Koenig, J. Blackwell, Biopolymers. **14**, 1885. (1975).
- [14] B. Kumar, K. Smita, L. Cumba, A., Debut R.N. Pathak. Bioinorganic Chemistry and Applications. doi: 10.1155/2014/784268. (2014).
- [15] S. Palanikumar, L. Kannamma, B. Meenarathi, R. Anbarasan, Int Nano Lett.

4(104). Doi: 10.1007/s40089-014-0104-9(2014).

- [16] B. Ajitha, A. Divya, G. S. Harish, P. Sreedhara Reddy, Research Journal of Physical Sciences. **1**(7), 11 (2013).
- [17] M. Jafari, A. Sobhani, M. Salavati-Niasari, J. Ind. Eng. Chem. 1-5. doi:10.1016/j.jiec.2013.12.078. (2014).
- [18] S. Ravikumar, R. Gokulakrishnan, International Journal of Pharmaceutical Sciences and Drug Research. **4**(2), 157 (2012).